

Structure and stability of charged clusters

Mark A. Miller

University Chemical Laboratory, Lensfield Road, Cambridge CB2 1EW, United Kingdom

E-mail: mam1000@cam.ac.uk

David A. Bonhommeau

GSMA UMR7331, Université de Reims Champagne-Ardenne, UFR Sciences Exactes et Naturelles, Moulin de la Housse B.P. 1039, 51687 Reims Cedex 2, France

Christopher J. Heard

School of Chemistry, University of Birmingham, Edgbaston, Birmingham B15 2TT, United Kingdom

Yuyoung Shin

University Chemical Laboratory, Lensfield Road, Cambridge CB2 1EW, United Kingdom

Riccardo Spezia

Université d'Evry val d'Essonne, LAMBE CNRS UMR8587, Blvd F. Mitterrand, Bât Maupertuis, 91025 Evry, France

Marie-Pierre Gaigeot

Université d'Evry val d'Essonne, LAMBE CNRS UMR8587, Blvd F. Mitterrand, Bât Maupertuis, 91025 Evry, France

Institut Universitaire de France (IUF), 103 Blvd St Michel, 75005 Paris, France

E-mail: mgaigeot@univ-evry.fr

Abstract. When a cluster or nanodroplet bears charge, its structure and thermodynamics are altered and, if the charge exceeds a certain limit, the system becomes unstable with respect to fragmentation. Some of the key results in this area were derived by Rayleigh in the nineteenth century using a continuum model of liquid droplets. Here we revisit the topic using a simple particle-based description, presenting a systematic case study of how charge affects the physical properties of a Lennard-Jones cluster composed of 309 particles. We find that the ability of the cluster to sustain charge depends on the number of particles over which the charge is distributed—a parameter not included in Rayleigh's analysis. Furthermore, the cluster may fragment before the charge is strong enough to drive all charged particles to the surface. The charged particles in stable clusters are therefore likely to reside in the cluster's interior even without considering solvation effects.

PACS numbers: 36.40.Wa, 07.05.Tp

1. Introduction

Charged clusters and small droplets are important in many areas of physical chemistry, ranging from aerosol formation in the atmosphere [1] to electrospray processes in the laboratory [2]. The presence of charge on a droplet affects both its interactions with other species and the physical properties of the individual droplet. Amongst the most important questions relating to physical properties are how much charge a cluster or droplet can accommodate without becoming unstable on short timescales, and how the break-up of the droplet proceeds as this charge limit is approached and exceeded.

One area where such considerations are crucial is electrospray ionisation mass spectrometry. The electrospray technique produces a stream of charged droplets that solvate molecules or complexes to be conveyed into the mass spectrometer for analysis. Before the analyte’s mass-to-charge ratio is measured, it becomes separated from the solvent, and some of the droplet’s charge is deposited on it. Various models have been proposed to describe the mechanism by which the solvent leaves the analyte [3, 4, 5] in different circumstances. Computer simulations with atomistic detail have been employed to obtain a more explicit picture of the desolvation process and also to study the structure of water droplets containing ions [6, 7, 8] and solvated biomolecules [9, 10, 11, 12].

On the fundamental question of the stability of pure charged droplets, the key theoretical work dates back well over a hundred years to Rayleigh [13], who considered arbitrary deformations of a uniformly charged, structureless spherical droplet. Deformations away from a spherical shape increase the surface area of the droplet, thereby increasing its surface energy, but at the same time decrease the electrostatic repulsion by spreading the charge out. At a total charge

$$Q_R = \pi\sqrt{8\epsilon_0\gamma D^3}, \quad (1)$$

known as the Rayleigh limit, the electrostatic contribution to the energy overwhelms the surface energy and the droplet becomes mechanically unstable. In Eq. (1), γ is the surface tension of the liquid, ϵ_0 is the vacuum permittivity and D is the droplet diameter. Rayleigh’s formula remains of great practical use to the present day.

To examine the nature of charge-driven instabilities with particle-level detail, simulations of small charged clusters have been carried out by adding Coulomb interactions to simple generic potentials like Lennard-Jones [14] and Morse [15]. However, these studies have mostly concentrated on total charges where the cluster is decisively in the unstable regime and rapidly undergoes fragmentation.

In this article, we take a closer look at the properties of charged clusters with an explicit but generic representation of individual particles, concentrating on the structure of clusters as the charge-driven instability is approached from below. We treat the clusters at equilibrium, setting aside the dynamical aspects of fragmentation for now. The results presented here constitute a case study on a cluster of 309 Lennard-Jones particles to which Coulomb repulsion has been added. 309 is a “magic number” for the Lennard-Jones potential; the lowest-energy structure consists of four

complete icosahedral shells around a central atom [16]. The present study represents the preliminary steps in a more comprehensive ongoing investigation of charged droplets.

2. Model and methods

Our cluster of $N = 309$ particles is bound by the pairwise potential

$$V = 4u \sum_{i < j}^N \left[\left(\frac{\sigma}{r_{ij}} \right)^{12} - \left(\frac{\sigma}{r_{ij}} \right)^6 \right] + \sum_{i < j}^N \frac{q_i q_j}{4\pi\epsilon_0 r_{ij}}, \quad (2)$$

where u and σ are the Lennard-Jones pair well-depth and diameter, respectively, r_{ij} is the separation of particles i and j , and q_i is the charge on particle i . By defining a reduced charge $q_i^* = q_i / (4\pi\epsilon_0\sigma u)^{1/2}$, along with the usual Lennard-Jones reduced energy and lengths $V^* = V/u$ and $r_{ij}^* = r_{ij}/\sigma$, Eq. (2) may be rewritten in the dimensionless form

$$V^* = \sum_{i < j}^N \left[4(r_{ij}^{*-12} - r_{ij}^{*-6}) + q_i^* q_j^* / r_{ij}^* \right].$$

We will consider clusters where n of the particles carry a charge $q_i^* = q^*$ and the remaining $N - n$ particles are uncharged, making the overall charge on the cluster $Q^* = nq^*$. Although q itself should be an integer multiple of the electronic charge e , the reduced charge q^* also depends on the Lennard-Jones parameters. We will therefore treat q^* as a continuously variable effective charge. The fact that the particles constituting the cluster are represented explicitly and may each carry a charge of only q^* or 0 means that there is no need to consider an underlying continuum medium with its own conductivity. The charge distribution is completely determined by the function V^* and a small number of external parameters, such as the temperature. Therefore, although our model is coarse-grained, its particulate nature makes it more physically detailed than a continuum model.

We simulate the cluster at thermodynamic equilibrium using canonical Monte Carlo (MC) simulations. In addition to standard displacements of individual particles, we employ trial moves that attempt to swap the charges on randomly chosen charged–uncharged pairs of particles while keeping all positions fixed. These steps are accepted according to the usual Metropolis criterion [17]. The swap moves are not intended to mimic the dynamical process of charge transfer or conductivity that may occur between molecules in certain systems. In particular, the swaps are not restricted to pairs of adjacent particles. The purpose of the moves is to enhance the efficiency with which the equilibrium distribution of charges is reached and sampled, and the moves achieve this by, in effect, decoupling the mobility of the charge from the movement of individual particles. The same distribution would eventually be achieved by any set of MC moves that obey (detailed) balance.

We will be concerned with the behaviour of the cluster as a function of the magnitude of the single-particle charge q^* for a given n and, to some extent, on the properties with a given charge as a function of temperature T . To accelerate sampling

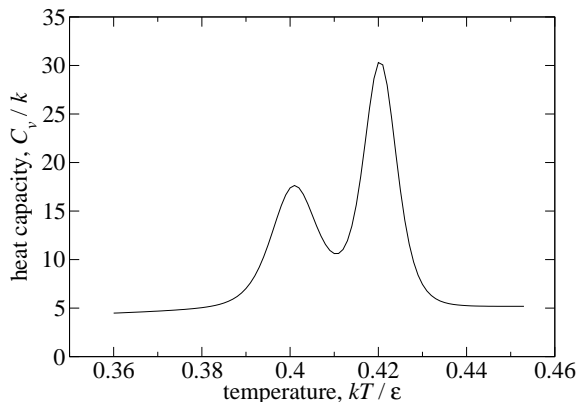


Figure 1. Heat capacity of the neutral LJ₃₀₉ cluster, obtained by the multiple histogram method.

in these cases, we have employed replica-exchange MC [18], using either the temperature [19] or the charge as the parameter that varies between replicas. In the latter case, the acceptance criterion for exchanging configurations \mathbf{X}_1 and \mathbf{X}_2 that are initially found in replicas where the single-particle charges are q_a^* and q_b^* , respectively, is

$$p^{\text{acc}} = \min \left\{ 1, \exp \left[(W(\mathbf{X}_1) - W(\mathbf{X}_2)) (q_a^{*2} - q_b^{*2}) / kT \right] \right\}.$$

Here, k is Boltzmann's constant and $W(\mathbf{X}) = \sum_{i < j}^n r_{ij}^{*-1}$, where the sum runs over pairs of charged particles.

Any cluster is thermodynamically unstable with respect to vaporisation unless it is confined. We therefore constrain the cluster to lie within a spherical container of radius $R = 6.5\sigma$ whose centre follows the centre-of-mass of the cluster [20]. This radius is large enough not to inhibit large fluctuations in the shape of the cluster and also allows fragmentation to occur. We shall return to the consequences of this particular choice of radius when discussing the results.

3. Stability

We will consider the effect of adding charge to the Lennard-Jones cluster at reduced temperatures $T^* = kT/u = 0.2$ and 0.43 . Figure 1 shows the canonical constant-volume heat capacity C_v of the cluster, derived from temperature replica-exchange simulations coupled with multiple histogram reweighting [21, 22]. The taller of the two peaks is due to the main melting transition [23], meaning that our two temperatures correspond to well within the solid-like state and just within the liquid-like regime, respectively.

At $T^* = 0.2$, the neutral cluster fluctuates uneventfully about its icosahedral global minimum [16]. This qualitative behaviour persists if some charge is added, but for sufficiently large charge, a small number of charged particles are expelled, leaving a well-defined sub-cluster at the centre of the spherical container. The expelled particles typically lie close to the container edge, repelled there by the long range Coulomb potential. We may therefore count an individual configuration as dissociated if at least

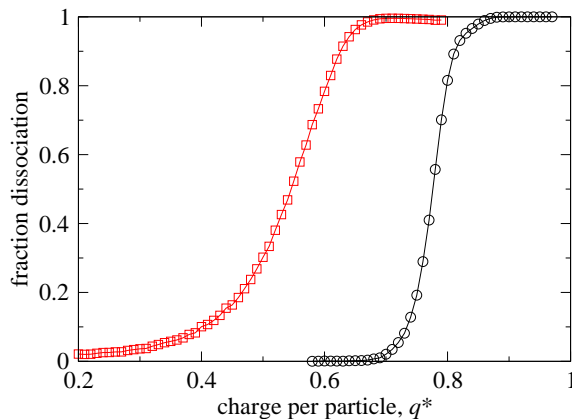


Figure 2. (Colour online) Fraction of configurations in which dissociation is detected for LJ₃₀₉ with $n = 100$ charged particles at temperatures $T^* = 0.2$ (black circles) and 0.43 (red squares) as a function of the charge per particle.

one charged particle lies within a small distance, chosen to be $\sigma/2$, from the container wall. The line marked with circles in Fig. 2 shows that the equilibrium fraction of dissociated configurations at equilibrium rises sharply at a particular value of the single-particle charge, indicating that electrostatic repulsion has become strong enough to overcome the cohesive part of the Lennard-Jones potential. We will designate the total charge at which the fraction of dissociated configurations passes through 0.5 by Q_{\max} ; beyond this threshold, more than half the equilibrium configurations are dissociated.

At the liquid-like temperature $T^* = 0.43$, a similar pattern is observed, as shown by the squares in Fig. 2. However, since the cluster has now escaped the basin of attraction of its icosahedral global minimum and explores a range of disordered structures, the transition from an intact cluster to full dissociation is a broader function of the charge. We will nevertheless use the same criterion of Q_{\max} to quantify the maximum charge that the cluster can sustain.

Importantly, Q_{\max} is a function of n , *i.e.* the maximum total charge that the cluster can sustain depends on the number of particles over which the charge is spread. Figure 3 shows that Q_{\max} increases quite dramatically with n , especially at the lower temperature. It is not straightforward to compare the Q_R of Eq. (1) with Q_{\max} , not least because we must work at temperatures well below the triple point of $T^* = 0.694$ [24], where the bulk surface tension is not known. However, we note that the influence of n discrete charges does not enter into Rayleigh’s analysis because in that analysis the droplet is treated as being homogeneously charged. The dependence of the maximum charge on n is potentially important in the context of small electrospray droplets, where the charge of the droplet may be due to a relatively small number of ions. Our thermodynamically based Q_{\max} suggests that such droplets have a greater tendency to dissociate by the emission of charged particles than a hypothetical cluster where the same amount of charge is spread out over a larger number of particles.

Increasing the container radius R decreases the value of Q_{\max} that is obtained

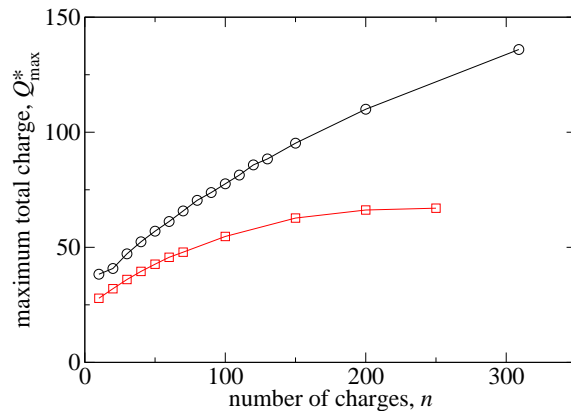


Figure 3. (Colour online) Maximum total charge Q_{\max}^* that the cluster can sustain at $T^* = 0.2$ (black circles) and $T^* = 0.43$ (red squares) as a function of particles n over which the charge is spread.

because dissociated charged particles can then go further from the remaining sub-cluster, thereby lowering the potential energy of the configuration and raising its statistical weight relative to the undissociated cluster. However, the decisive trend of increasing Q_{\max} with n persists for all R large enough to permit dissociation.

If the charge is increased beyond Q_{\max} , a further structural change may result. It is possible for the cluster to split into two or more large sections, which then repel each other as far as the container will allow. This subdivision does not happen if n is sufficiently small since the electrostatic energy can then be lowered by the emission of individual particles without sacrificing the attractive Lennard-Jones interactions in the main part of the cluster. However, as n increases, subdivision occurs at a threshold increasingly close to Q_{\max} and, for large container radius, may even preempt significant loss of individual charged particles. This observation again points to the importance of taking into account not only the total charge borne by a cluster but also the number of particles over which the charge is divided. One may anticipate that a dynamic study would find increased competition between different instability mechanisms at higher n .

4. Structure

An important question concerning charged droplets is where the charged particles reside. In the case of ions dissolved in water, highly specific effects come into play in determining the affinity of ions for the surface of the bulk liquid itself, according to how a given ion influences the interactions between the water molecules [25, 26]. In a droplet and in the absence of strong surface affinity effects, one might expect ions to be mutually repelled to the droplet surface by electrostatic considerations. However, this is not always found to be the case [27, 7].

Our model is more straightforward and generic than water, allowing us to consider the structure of charged droplets without the rather special effects of hydrogen bonding. Energetically, the driving forces in our model are towards the optimisation of as many

Lennard-Jones pairwise neighbours as possible and toward the maximisation of distance between like charges. The global potential energy minimum structure of the cluster, obtained using the basin hopping algorithm [28] is always a slightly relaxed version of the neutral icosahedron [16]. As n is increased from small values, the charged particles preferentially occupy vertices, then edges and finally faces of the outer shell before populating the cluster’s interior. Counteracting these energetic tendencies at finite temperature is the entropy of permuting charged and neutral particles.

To determine how the charges are divided between the surface and the interior of the cluster, we need a method for identifying surface particles. At solid-like temperatures, where the cluster retains a clear structure of concentric shells, the outermost shell of 162 particles can unambiguously be designated as the surface. For liquid-like structures, the surface is less clear-cut and its curvature adds to the difficulty of devising a simple algorithm to detect the outermost layer. Existing methods to tackle this problem include the cone algorithm of Dellago and coworkers [29], which identifies surface particles as those for which the vertex of a cone with a particular aperture can be placed at the particle’s centre without any other particles falling inside the cone. The cone may have any orientation, thereby taking into account the fact that the surface normal of a droplet may locally deviate significantly from the vector joining that region to the droplet’s centre.

We have devised a somewhat more straightforward algorithm that shares the advantageous features of the cone algorithm and produces a reliable and intuitively realistic division between surface and core particles. The method borrows an idea from algorithms used to determine the surface of proteins [30]. The principle is that a particle should be regarded as lying on the surface if it would be accessible by a fictitious probe particle approaching from a distance, while the cluster configuration is held fixed. To determine this accessibility, a nominal hard-sphere diameter D_{LJ} is assigned to the Lennard-Jones particles. We then attempt to place a probe particle of diameter D_{pr} in contact with any combination of three particles that are sufficiently close for three contacts to be achieved simultaneously. For each such triplet, there are two possible positions for the probe particle, located symmetrically on either side of the plane defined by the triplet on the line passing through the circumcentre of the triangle. If the probe particle in at least one of these positions does not overlap with any other particle in the cluster then all three Lennard-Jones particles are designated as lying on the surface. A given particle may qualify as being on the surface by being tested in conjunction with any two of its neighbours. Although a systematic test over all triplets of particles may seem computationally expensive, it is quite easy to omit needless iterations of the outer loops, and neighbour lists [31] could be implemented for efficiency in larger systems if necessary.

The only parameters to fix in this probe method are the nominal diameters D_{LJ} and D_{pr} . Both should be comparable with σ and the results should not be sensitive to the values chosen. We have found that choosing a slightly smaller probe diameter enables the algorithm to cope better with crevices in the surface and adopted $D_{\text{LJ}} = 1.2\sigma$,

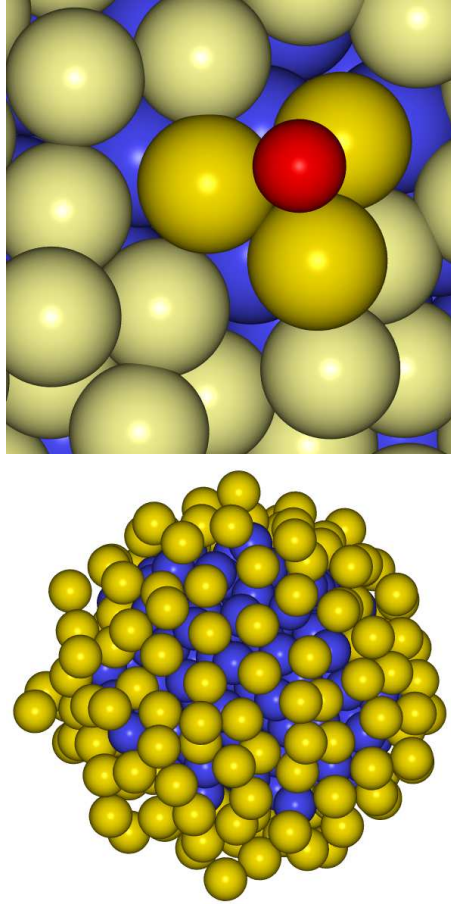


Figure 4. (Colour online) Top: Illustration of the method for distinguishing surface particles (light/yellow) from the core of the cluster (dark/blue). The surface particles touching the probe (small, red) are highlighted. Bottom: liquid-like snapshot of the cluster, highlighting the surface particles.

$D_{\text{pr}} = 0.8\sigma$ in this study. The probe method and an example of its outcome are illustrated in Fig. 4.

Figure 5 shows how the average number of charged particles occupying surface sites varies with the magnitude of the charge for several values of n at $T^* = 0.43$. Due to the liquid-like structure, the number of surface sites fluctuates and the sites have to be identified for each sample separately. The charge on the horizontal axis of the plot has been scaled by the maximum charge that the cluster can sustain for each value of n respectively (Fig. 3). Looking at the vertical line Q^*/Q_{max}^* shows that it is only for very small numbers of charges and only when the charge approaches the limit of stability of the droplet that one finds most of the charged particles on the surface of the cluster. Hence, for a cluster of this size bound by the generic Lennard-Jones potential, the charge required to drive the majority of particles electrostatically to the cluster surface is already too much for the cluster itself to remain intact. Therefore, even in a model without specific surface affinity effects or polarisability, charged particles may be found predominantly in the interior of the cluster.

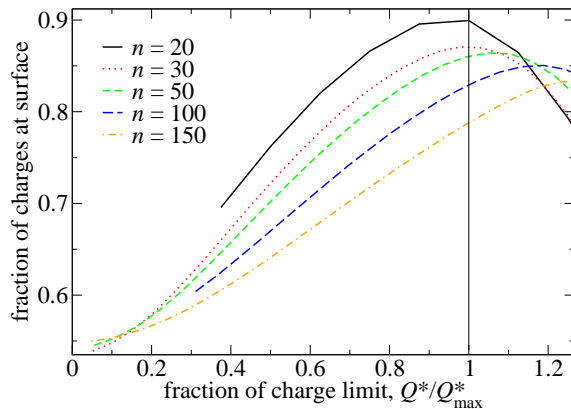


Figure 5. (Colour online) The fraction of charges that occupy surface sites as a function of the total charge of the cluster for different numbers n of charged particles at temperature $T^* = 0.43$. For each value of n , the charge axis has been scaled by the maximum charge from Fig. 3. The vertical line highlights the limit $Q^* = Q_{\max}^*$.

For $Q^* > Q_{\max}^*$, the loss of charged particles from the cluster causes the number of charges at the surface to start decreasing for small n in Fig. 5. However, for higher n , although some charged particles are expelled, the higher charge still leads to an overall increase in the proportion of charges driven to the surface of the remaining sub-cluster, and the upward trend continues beyond Q_{\max}^* .

In our simple model, the occupation of surface sites by charged particles is determined by a competition between electrostatic repulsion of charges to the surface and the entropy of mixing of charged and uncharged particles. For solid-like temperatures, the balance between these effects can be calculated quite accurately with little effort by using a few approximations. At these low temperatures, let us neglect the effect of thermal fluctuations on the positions of the particles and consider the structure to be the perfect icosahedron of the neutral cluster's global potential energy minimum, which has $S = 162$ surface particles. If n of the $N = 309$ particles are charged, the number of ways of permuting s of them amongst the surface sites and the remaining $n - s$ amongst the $N - S$ core sites is

$$\Omega_{N,n}(s) = C_s^S C_{(n-s)}^{(N-S)},$$

where $C_b^a = a!/[b!(a-b)!]$ is a binomial coefficient. Let us also define

$$W_{N,n}(s) = \left\langle \sum_{i<j}^n r_{ij}^{*-1} \right\rangle_s, \quad (3)$$

where the sum runs over the charged particles only and the angle brackets imply an unweighted average over configurations in which s charges are randomly assigned to surface sites in the frozen cluster and the remaining charges are randomly distributed amongst the core sites. $W_{N,n}(s)$ can be sampled very quickly since the particle positions are held fixed while the charges are permuted amongst the sites, and the reciprocal pairwise distances need be calculated only once. The mean energy of configurations

with s charges at surface sites is then given instantly for any magnitude of the charge by

$$\bar{V}_{N,n}^*(s) = q^{*2}W_{N,n}(s).$$

We may therefore predict the probability that precisely s particles lie on surface sites to be

$$p_{N,n}(s) \propto \Omega_{N,n}(s) \exp \left[-\bar{V}_{N,n}^*(s)/kT \right], \quad (4)$$

with the constant of proportionality defined by the normalisation $\sum_{s=0}^n p_{N,n}(s) = 1$.

Figure 6 compares the predictions of Eq. (4) with the results of explicit MC simulations. The averages for $W_{N,n}(s)$ in Eq. (3) were made using 10^5 samples at each value of s , which allows $W_{N,n}(s)$ to be evaluated in a matter of seconds for the full range of s . At low n and modest Q^*/Q_{\max}^* , the predictions of Eq. (4) compare essentially perfectly with the simulations even at $T^* = 0.3$, which is approaching the first peak in the heat capacity (Fig. 1). As n increases, Eq. (4) begins to overestimate the number of charged particles at the surface, but the peak position is only in error by a few per cent, even for $n = 150$ and a total charge approaching Q_{\max} . Given that $\bar{V}_{N,n}^*$ is a crude average and that thermal motion and charge-induced distortion of the cluster are neglected in Eq. (4), the simple and fast prediction works well. Importantly, we may conclude that the opposing driving forces of electrostatic repulsion and the permutational entropy capture most of the effects that determine the location of the charges in this model at low temperatures.

In principle, a similar approach could be taken to the liquid-like state. However, the number of surface sites is then no longer fixed and it may be necessary to sample a selection of disordered structures. Furthermore, we may anticipate that the presence of charge will have a greater influence in distorting the cluster from its neutral shape than it does in the solid-like regime. We are currently investigating the influence of these effects.

We conclude this section by noting that in some systems there may be more sophisticated mechanisms that affect the equilibrium distribution of charges. For example, the surface of liquid water may develop a slight excess charge even without dissolved ions due to the asymmetry of hydrogen bonds, which results in a small transfer of charge between molecules [32, 33]. A related effect can lead to some of the charge of a solvated ion appearing near the water surface via a chain of partial charge transfers through oriented water molecules [7]. Hence, some of the *charge* may appear at the surface even though the *ions* are located within the bulk liquid. Our simple Lennard-Jones model does not attempt to capture the structure of water or the rather specific effects associated with hydrogen bonding. However, the model could be modified to incorporate some degree of charge separation within individual particles by adding a polarisability term to the potential. Self-consistent solution of the polarisability equations to obtain the induced dipole moments adds a considerable computational overhead to the simulations. Some preliminary calculations of this sort reveal, as

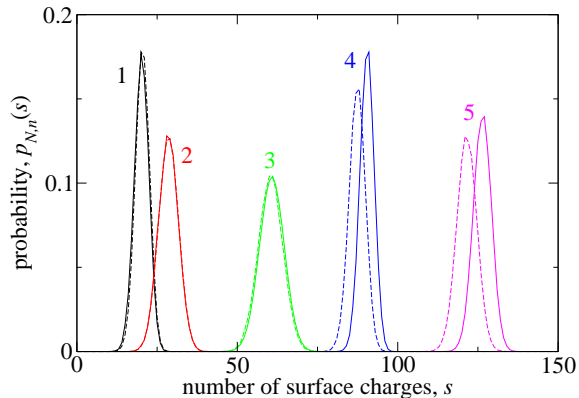


Figure 6. Probability distributions of the number of charged particles lying on the cluster surface for various combinations of parameters as listed in the legend. For each pair of curves, the solid line is from explicit MC calculations while the dashed line is the prediction of Eq. (4). The five sets of data correspond to the following parameters:

- 1: $n = 30$, $q^* = 0.33$, $T^* = 0.2$, $Q^*/Q_{\max}^* = 0.28$
- 2: $n = 50$, $q^* = 0.16$, $T^* = 0.3$, $Q^*/Q_{\max}^* = 0.20$
- 3: $n = 100$, $q^* = 0.14$, $T^* = 0.2$, $Q^*/Q_{\max}^* = 0.26$
- 4: $n = 100$, $q^* = 0.44$, $T^* = 0.2$, $Q^*/Q_{\max}^* = 0.80$
- 5: $n = 150$, $q^* = 0.336$, $T^* = 0.2$, $Q^*/Q_{\max}^* = 0.80$

expected, that polarisability leads to an even lower tendency of charged particles to lie at the surface of the droplet.

5. Concluding remarks

We have taken a thermodynamic approach to the stability and structure of the 309-particle Lennard-Jones cluster bearing charge on some of the particles. By confining the cluster to a spherical container we have calculated the equilibrium between intact and dissociated configurations and have obtained statistics for the occupation of surface sites by charged particles.

The key observation from this work is that both the stability of the cluster and the extent to which charges are likely to be found at its surface depend not just on the total charge but also on the number of particles over which the charge is distributed. When the charge is spread over more particles, the cluster is able to sustain a greater total charge but the fraction of the charges that reside at surface sites is lower. In general, the cluster is prone to break up at charges lower than those required to drive all the charged particles to the surface.

The location of charged particles in a sphere became an important topic following the introduction of the “plum pudding” model of the atom by Thomson in 1904 [34]. Since then, the “Thomson problem” has come to refer to finding the energetically optimal distribution of point charges constrained to the surface of a sphere. This idealised model has received considerable attention as an interesting exercise in global optimisation [35]. Although our charged Lennard-Jones cluster seems to share some

common features with the Thomson problem, we note that the charged particles would only be free to move continuously on the cluster surface when the cluster has melted, since at low temperatures the charges would be constrained to lie at the sites of the icosahedral structure. However, at liquid-like temperatures we have seen that the charges do not all reside at the surface of the sphere and that entropy plays a large role in determining their distribution. This means that it is not easy to make contact with the Thomson problem in this context.

Returning to the original motivation of a better understanding of electrospray ionisation, it will now be essential to move to a dynamical treatment of cluster instability and the mechanisms of fragmentation. An unconfined cluster undergoes evaporation even of neutral particles, which would have the effect of concentrating charge within a shrinking cluster. It will therefore be important to approach the instability from below as well as looking at the highly-charged regime. The Lennard-Jones model should allow such processes to be investigated in detail for a cluster bound by simple interactions. We intend to develop this coarse-grained approach in a number of directions, including inhomogeneous droplets in which a solute has been introduced.

Acknowledgments

MAM thanks EPSRC (U.K.) for financial support. DAB acknowledges support from Génopôle-Evry for postdoctoral funding as well as the supercomputing centre of Champagne-Ardenne (ROMEO) for computational resources and technical support. MPG is grateful to Churchill College, Cambridge (U.K.) and the French Foreign Office for an Overseas Fellowship. Travel associated with this collaboration was supported by the Alliance Programme of the British Council and the French Ministère des Affaires Étrangères. The authors thank Dr Florent Calvo, Prof. Daan Frenkel and Dr Benjamin Rotenberg for helpful discussions.

References

- [1] A. Hirsikko, T. Nieminen, S. Gangné, K. Lehtipalo, H. E. Manninen, M. Ehn, U. Hörrak, V.-M. Kerminen, L. Laakso, P. H. McMurry, A. Mirme, T. Petäjä, H. Tammet, V. Vakkari, M. Vana, and M. Kulmala. Atmospheric ions and nucleation: a review of observations. *Atmos. Chem. Phys.*, 11:767–798, 2011.
- [2] J. B. Fenn. Electrospray wings for molecular elephants (Nobel lecture). *Angew. Chem. Int. Ed.*, 42:3871–3894, 2003.
- [3] M. Dole, L. L. Mack, R. L. Hines, R. C. Mobley, L. D. Ferguson, and M. B. Alice. Molecular beams of macroions. *J. Chem. Phys.*, 49:2240–2249, 1968.
- [4] J. V. Iribarne and B. A. Thomson. On the evaporation of small ions from charged droplets. *J. Chem. Phys.*, 64:2287–2294, 1976.
- [5] L. Konermann. A simple model for the disintegration of highly charged solvent droplets during electrospray ionization. *J. Am. Soc. Mass Spectrom.*, 20:496–506, 2009.
- [6] E. Ahadi and L. Konermann. Molecular dynamics simulations of electrosprayed water nanodroplets: Internal potential gradients, location of excess charge centers, and “hopping” protons. *J. Phys. Chem. B*, 113:7071–7080, 2009.

- [7] E. Ahadi and L. Konermann. Surface charge of electrosprayed water nanodroplets: A molecular dynamics study. *J. Am. Chem. Soc.*, 132:11270–11277, 2010.
- [8] K. Ichiki and S. Consta. Disintegration mechanisms of charged aqueous nanodroplets studied by simulations and analytical models. *J. Phys. Chem. B*, 110:19168–19175, 2009.
- [9] S. Consta. Manifestation of Rayleigh instability in droplets containing multiply charged macroions. *J. Phys. Chem. B*, 114:5263–5268, 2010.
- [10] I. Marginean, V. Znamenskiy, and A. Vertes. Charge reduction in electrosprays: Slender nanojets as intermediates. *J. Phys. Chem. B*, 110:6397–6404, 2006.
- [11] M. Z. Steinberg, R. Elber, F. W. McLafferty, R. B. Gerber, and K. Breuker. Early structural evolution of native cytochrome c after solvent removal. *ChemBioChem*, 9:2417–2423, 2008.
- [12] A. Patriksson, E. Marklund, and D. van der Spoel. Protein structures under electrospray conditions. *Biochemistry*, 46:933–945, 2007.
- [13] Lord Rayleigh. On the equilibrium of liquid conducting masses charged with electricity. *Philos. Mag.*, 14:184–186, 1882.
- [14] M. J. Ison and C. O. Dorso. Role of Coulomb interaction in fragmentation. *Phys. Rev. C*, 69:027001, 2004.
- [15] Y. Levy, I. Last, and J. Jortner. Dynamics of fission and Coulomb explosion of multicharged large finite systems. *Mol. Phys.*, 104:1227–1237, 2006.
- [16] D. Romero, C. Barrón, and S. Gómez. The optimal geometry of Lennard-Jones clusters: 148–309. *Comp. Phys. Comm.*, 123:87–96, 1999.
- [17] D. Frenkel and B. Smit. *Understanding Molecular Simulation*. Academic Press, San Diego, 2nd edition, 2002.
- [18] C. J. Geyer and E. A. Thompson. Annealing Markov chain Monte Carlo with applications to ancestral inference. *J. Am. Stat. Assoc.*, 90:909–920, 1995.
- [19] J. P. Neirotti, F. Calvo, D. L. Freeman, and J. D. Doll. Phase changes in 38-atom Lennard-Jones clusters. I. A parallel tempering study in the canonical ensemble. *J. Chem. Phys.*, 112:10340–10349, 2000.
- [20] J. K. Lee, J. A. Barker, and F. F. Abraham. Theory and Monte Carlo simulation of physical clusters in the imperfect vapor. *J. Chem. Phys.*, 58:3166–3180, 1973.
- [21] P. Labastie and R. L. Whetten. Statistical thermodynamics of the cluster solid–liquid transition. *Phys. Rev. Lett.*, 65:1567–1570, 1990.
- [22] S. Weerasinghe and F. G. Amar. Absolute classical densities of states for very anharmonic systems and applications to the evaporation of rare gas clusters. *J. Chem. Phys.*, 98:4967–4983, 1993.
- [23] E. G. Noya and J. P. K. Doye. Structural transitions in the 309-atom magic number Lennard-Jones cluster. *J. Chem. Phys.*, 124:104503, 2006.
- [24] E. A. Mastny and J. J. de Pablo. Melting line of the Lennard-Jones system, infinite size, and full potential. *J. Chem. Phys.*, 127:104504, 2007.
- [25] C. Caleman, J. S. Hub, P. J. van Maaren, and D. van der Spoel. Atomistic simulation of ion solvation in water explains surface preference of halides. *Proc. Natl. Acad. Sci. USA*, 108:6838–6842, 2011.
- [26] H. Takahashi, K. Maruyama, Y. Karino, A. Morita, M. Nakano, P. Jungwirth, and N. Matubayasi. Energetic origin of proton affinity to the air/water interface. *J. Phys. Chem. B*, 115:4745–4751, 2011.
- [27] V. Znamenskiy, I. Margineau, and A. Vertes. Solvated ion evaporation from charged water nanodroplets. *J. Phys. Chem. A*, 107:7406–7412, 2003.
- [28] D. J. Wales and J. P. K. Doye. Global optimization by basin-hopping and the lowest energy structures of Lennard-Jones clusters containing up to 110 atoms. *J. Phys. Chem. A*, 101:5111–5116, 1997.
- [29] Y. Wang, S. Teitel, and C. Dellago. Melting of icosahedral gold nanoclusters from molecular dynamics simulations. *J. Chem. Phys.*, 122:214722, 2005.
- [30] F. M. Richards. Areas, volumes, packings and protein structures. *Ann. Rev. Biophys. Bioeng.*,

- 6:151–176, 1977.
- [31] M. P. Allen and D. J. Tildesley. *Computer Simulation of Liquids*. Clarendon Press, Oxford, 1987.
 - [32] R. Vácha, S. W. Rick, P. Jungwirth, A. G. F. de Beer, H. B. de Aguiar, J.-S. Samson, and S. Roke. The orientation and charge of water at the hydrophobic oil droplet–water interface. *J. Am. Chem. Soc.*, 133:10204–10210, 2011.
 - [33] R. Vácha, O. Marsalek, A. P. Willard, D. J. Bonhuis, R. R. Netz, and P. Jungwirth. Charge transfer between water molecules as the possible origin of the observed charging at the surface of pure water. *J. Phys. Chem. Lett.*, 3:107–111, 2011.
 - [34] J. J. Thomson. On the structure of the atom. *Philos. Mag. Ser. VI*, 39:237–265, 1904.
 - [35] D. J. Wales and S. Ulker. Structure and dynamics of spherical crystals characterized for the Thomson problem. *Phys. Rev. B*, 74:212101, 2006.